

COORDINATION COMPOUNDS

Structure of Potassium and Cesium Barbiturates

N. N. Golovnev^{a,*}, M. S. Molochev^{a,b,c}, and M. K. Lesnikov^a

^aSiberian Federal University, Krasnoyarsk, 660041 Russia

^bKirenskii Institute of Physics, Siberian Branch, Russian Academy of Sciences, Krasnoyarsk, 660036 Russia

^cFar Eastern State Transport University, Khabarovsk, 680021 Russia

*e-mail: ngolovnev@sfu-kras.ru

Received November 22, 2017

Abstract—The structures of *catena*-[K(μ_6 -Hba-O,O,O',O',O'')] (**I**) and *catena*-[Cs(μ_6 -Hba-O,O,O',O',O',O'')] (**II**), where H₂ba is barbituric acid C₄H₄N₂O₃, were characterized by powder X-ray diffraction. Crystallographic data: $a = 14.1603$ (4) Å, $b = 3.68977$ (9) Å, $c = 10.9508$ (3) Å, $\beta = 82.226$ (1)°, $V = 566.90$ (3) Å³, space group $P2_1/n$, $Z = 4$ for **I**; $a = 14.652$ (1) Å, $b = 11.7275$ (7) Å, $c = 3.8098$ (3) Å, $\beta = 79.140$ (6)°, $V = 642.90$ (8) Å³, space group $C2/m$, $Z = 4$ for **II**. The structural topologies of alkali metal complexes with barbituric acid and some its derivatives were compared. The thermal stability of complexes **I** and **II** in an air atmosphere was studied.

Keywords: potassium and cesium barbiturates, synthesis, structure, thermal decomposition

DOI: 10.1134/S0036023618100078

Barbituric acid (H₂ba) is the parent compound of an important class of analgesic medicines, namely, barbiturates [1]. As potentially polyfunctional N,N',O,O',O''-coordinated ligand, H₂ba is able to form complexes of various compositions with metal ions these complexes having useful functional properties. Acid H₂ba and its anion Hba⁻ can participate in numerous hydrogen bonds and are prone to self-association, which enriches their supramolecular chemistry [2]. From the structural viewpoint, barbiturate metal complexes are still poorly studied [3].

In this work, *catena*-(μ_6 -barbiturato-O,O,O',O',O'')potassium [K(μ_6 -Hba-O,O,O',O',O'')] (**I**) and *catena*-(μ_6 -barbiturato-O,O,O',O',O'')cesium [Cs(μ_6 -Hba-O,O,O',O',O'')] (**II**) have been synthesized. Their structure and thermal decomposition have been studied by powder X-ray diffraction. Potassium is present in the organism, so information about the structure of its barbiturate may be useful in medicine and pharmaceuticals.

EXPERIMENTAL

The synthesis of complexes **I** and **II** were performed using barbituric acid, KOH, and Cs₂CO₃, which were of chemically pure grade.

H₂ba (0.2 g, 1.6 mmol) was dissolved in water (3 mL) under heating (~90°C), thereupon the equimolar amount of KOH (0.09 g) was added to the hot solution. The resulting transparent solution (pH 6)

was slowly cooled to the room temperature. In 24 h, the solution with a white fine-crystalline precipitate was filtered out, washed with water (1 mL) and acetone (1 mL), and dried in air to a constant mass. Complex **I** (0.174 g) was thus synthesized with a yield of 66%.

The synthesis of complex **II** was performed by the same method, using Cs₂CO₃ instead of KOH at the molar ratio Cs₂CO₃ : H₂ba = 1 : 2. Complex **II** (0.202 g) was thus synthesized with a yield of 49%. However, we have not managed to separate single crystals of these complexes from an aqueous solution.

Thermal analysis of these complexes (8.79 mg of **I** and 9.18 mg of **II**) was performed on a TA Instruments SDT-Q600 analyzer (United States) in an air flow (50 mL/min) within a temperature range of 22–350°C at a heating rate of 10 K/min. The composition of evolved gases was determined on a Thermo Scientific Nicolet 380 IR spectrometer combined with a thermoanalyzer.

Powder X-ray diffraction analysis. The powder X-ray diffraction patterns of complexes **I** and **II** were recorded on a Bruker D8 ADVANCE diffractometer (linear VANTEC detector, CuK α radiation). In the course of experiment, different sizes of primary beam slits of 0.6 and 2 mm were selected within the 2 θ angle range 5°–70° and 70°–120°, respectively. The scanning step (0.016°) was constant within all ranges, and the exposure time at every step was 1.5 s for all ranges of angles. Afterwards, the standard deviations of intensities at all X-ray diffraction pattern points were calculated, thereupon the intensities and standard devia-

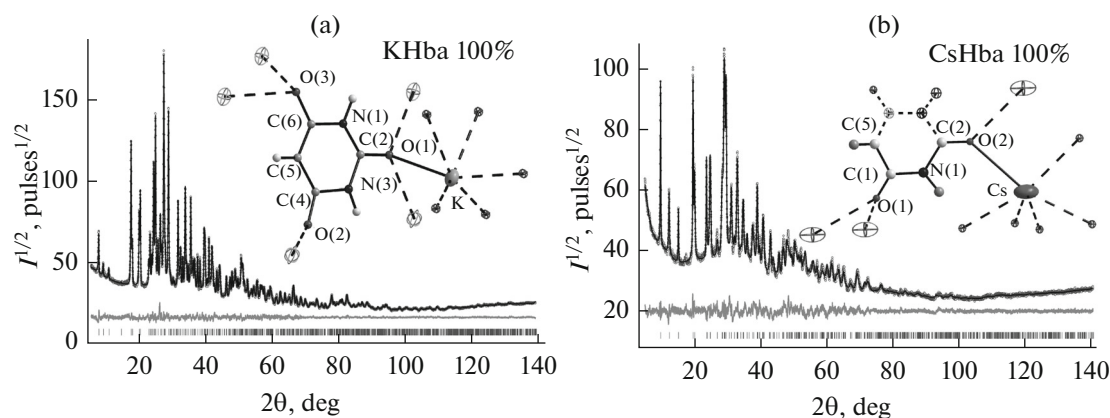


Fig. 1. Experimental (dots), theoretical (line), and difference (line below) powder X-ray diffraction patterns for crystals of (a) complex **I** and (b) complex **II** after Rietveld refinement and independent unit cell parts in their structures (inserts). Uncolored ellipsoids are the nearest bonded atoms, and chemical bonds between the atoms of the independent unit cell part and their neighboring atoms are shown as dashed lines. Ellipsoids of the thermal parameters of heavy ions are shown with a 50-% probability.

tions of all points in the large-angle range were multiplied by a normalizing coefficient of 0.3. Rietveld refinement implemented in the TOPAS 4.2 software [4] took into account the standard deviation of each point by introducing the weight of each point $w_i = 1/\sigma(I_i)^2$ into the least-squares technique. In this method, the weights of weak large-angle and strong small-angle reflections are equalized, while these weights in conventional experiment are not equivalent, and the experimental structural data contained in the large-angle of an X-ray diffraction pattern are less significant.

The positions of peaks in the X-ray diffraction patterns of complexes **I** and **II** were determined by the EVA program (2004 release) from the Bruker DIFFRAC-PLUS software suite. The unit cell parameters of complex **I** were determined by the TOPAS 4.2 software [4]. The search for these parameters has given a monoclinic unit cell with $a = 14.138 \text{ \AA}$, $b = 3.682 \text{ \AA}$, $c = 10.934 \text{ \AA}$, and $\beta = 82.21^\circ$ (GOOF(24) = 22.8). No non-indexed reflections have been revealed. The extinction laws have uniquely pointed to space group $P2_1/n$. The structures were solved by modeling in a straight space with further simulated annealing by the TOPAS 4.2 software. The unit cell volume corresponded to 9 or 10 non-hydrogen atoms in the independent part, i.e., one $C_4H_3N_2O_3^-$ ion (Hba^-) and one K^+ ion in the independent part of a unit cell. Simulated annealing gave the structural model in which the K^+ ion and all atoms of the Hba^- ion were in shared positions. This model was used to perform Rietveld refinement by the TOPAS 4.2 software. No restrictions were imposed on bond lengths and bond angles except the coordinates of H atoms in the Hba^- ion. The thermal parameter (TP) of the K^+ ion was refined in the anisotropic approximation, while the isotropic approximation was used to refine the thermal param-

eters of the other atoms. After refinement, all TPs had normal values. The selected crystallographic characteristics of complex **I** and the parameters of X-ray diffraction experiment are the following: $C_4H_3KN_2O_3$, $FW_r = 166.1782$, $a = 14.1603 (4) \text{ \AA}$, $b = 3.68977 (9) \text{ \AA}$, $c = 10.9508 (3) \text{ \AA}$, $\beta = 82.226 (1)^\circ$, $V = 566.90 (3) \text{ \AA}^3$, space group $P2_1/n$, $Z = 4$, $\rho_x = 1.947 \text{ g/cm}^3$, $\mu = 7.734 \text{ mm}^{-1}$, 2θ range of 5° – 140° , 1083 reflections, 94 refined parameters, $R_B = 1.00\%$, $R_{wp} = 3.29\%$, $R_{exp} = 1.93\%$, $R_p = 2.94\%$, $\chi^2 = 1.71$. The difference X-ray diffraction pattern and the independent unit cell part are shown in Fig. 1a.

The unit cell parameters and space group of complex **II** were determined by the TOPAS 4.2 software. The search for parameters has given a monoclinic base-centered unit cell with $a = 14.657 \text{ \AA}$, $b = 11.712 \text{ \AA}$, $c = 3.796 \text{ \AA}$, $\beta = 79.30^\circ$ (GOOF(23) = 18.3). The only weak reflection assigned by us to an admixture has remained unindexed. The analysis of reflection extinctions gave three possible space group variants: $C2$, Cm , and $C2/m$. First, it was decided to search the structure in the most highly symmetric space group $C2/m$. The structure was solved by modeling in a straight space with further annealing by the TOPAS 4.2 software. The unit cell volume corresponded to 4 or 5 non-hydrogen atoms in its independent part, thus meaning the arrangement of ions in special positions.

One $C_4H_3N_2O_3^-$ (Hba^-) ion and one Cs^+ ion were generated in the independent unit cell part. In this case, all the atoms had dynamic position occupancy [4, 5], which provide the possibility to consider several atoms residing in the same small area as a single atom. Simulated annealing gave the structural model in which the independent unit cell part contained half of the Cs^+ ions and half of the Hba^- ions. This model was used to perform Rietveld refinement by the TOPAS 4.2 software. No restrictions were imposed on bond

Table 1. Geometric characteristics of hydrogen bonds in the structures of complexes **I** and **II**

D–H···A	<i>d</i> , Å			DHA angle, deg	Symmetry codes for atom A
	D–H	H···A	D···A		
Structure of complex I					
N(1)–H(1)···O(3)	0.99(6)	1.81(5)	2.785(6)	168(4)	$-x, -y, 1 - z$
N(3)–H(3)···O(2)	0.88(6)	2.01(6)	2.795(5)	149(6)	$-x, 1 - y, -z$
Structure of complex II					
N(1)–H(1)···O(1)	1.03(3)	1.80(2)	2.83(2)	173(2)	$1/2 - x, 1/2 - y, 1 - z$

length and bond angles except the coordinates of H atoms in the Hba[−] ion. The thermal parameter of the Cs⁺ ion was refined in the anisotropic approximation, while the isotropic approximation was used to refine the thermal parameters of the other atoms; after refinement, all the atoms have normal values. Finally, it was decided to end with the model of space group *C2/m* and do not search the structure of space groups *C2* and *Cm*. A crystal of complex **II** has the following parameters: C₄H₃CsN₂O₃, FW_r = 259.9844, *a* = 14.652 (1) Å, *b* = 11.7275 (7) Å, *c* = 3.8098 (3) Å, β = 79.140 (6)°, *V* = 642.90 (8) Å³, space group *C2/m*, *Z* = 4, ρ_x = 2.686 g/cm³, μ = 44.478 mm^{−1}, 2θ range is 5°–140°, 651 reflections, 87 refined parameters, *R*_B = 1.99%, *R*_{wp} = 4.16%, *R*_{exp} = 2.22%, *R*_p = 3.67%, χ² = 1.87. The difference X-ray diffraction pattern and the independent unit cell part are shown in Fig. 1b.

The structures of complexes **I** and **II** were deposited with the Cambridge Structure Database (nos. 1554996 and 1554997, respectively). The results can be acquired at the website www.ccdc.cam.ac.uk/data_request/cif.

RESULTS AND DISCUSSION

The independent part of a unit cell of complex **I** contains the K⁺ cation and the Hba[−] anion (Fig. 1a). In the Hba[−] ion, the O1 atom is linked to three K⁺ ions, the O(2) ion is linked to one K⁺ ion, and the O(3) atom is bonded to two K⁺ ions. The range of K–O bond lengths is 2.741(4)–2.935(4) Å. K⁺ ion are located in the center of distorted tetrahedra (Figs. 2a and 2b) kinked into pairs by a shared edge. These pairs are bonded to each other via bridging Hba[−] ions to form a three-dimensional framework, where rings *r*(4) and *r*(12) (Fig. 2a), which are also typical for a number of metal complexes with 2-thiobarbituric acid (H₂tba) [6] and 1,3-diethyl-2-thiobarbituric acid (HDetba) [7, 8], can be distinguished. The intermolecular hydrogen bonds N–H···O (Table 1) linking Hba[−] ions into infinite chains along axis *c* (Fig. 2a) form six- and eight-membered rings (supramolecular motifs *S*(6)

and *R*₂²(8)), which are also present in the other metal complexes with H₂tba [9] and H₂tba [6].

The independent part of a unit cell of complex **II** contains half of the Cs⁺ ions and half of the Hba[−] ions. Symmetry plane *m* passes through the C(2) and C(5) atoms, multiplies the N(1), C(1), and O(1) atom positions, and thereby forms the complete Hba[−] ion (Fig. 1b). The C–O, C–N, and C–C bond lengths and the corresponding bond angles in Hba[−] coincide with the bond lengths and bond angles found in complex **I** and in the other compounds [9, 10]. In contrast to complex **I**, each O atom of the Hba[−] ion in complex **II** is linked to two metal cations (Fig. 1b). Like the K⁺ ion, the Cs⁺ ion is surrounded by the six O atoms of six Hba[−] anions at the vertices of a distorted tetrahedron. The Cs–O bond lengths (3.05(2)–3.14(2) Å) agree with the literature data [10]. Similarly to complex **I**, CsO₆ octahedra share their edges to form pairs linked via bridging Hba[−] ions into a three-dimensional framework (Figs. 2c and 2d). In one projection, the structures of KHba and CsHba are similar and have the same motifs (Figs. 2a and 2c). In the other projection, it is possible to see some distinctions (Figs. 2b and 2d) as the O(2) atom of the Hba[−] ion is coordinated to two metal ions in complex **II** and only one metal ion in complex **I** and, on the contrary, the O(1) atom is coordinated to a greater number of metal ions in complex **I** in comparison with complex **II**. Similarly to complex **I**, the hydrogen bonds N–H···O between Hba[−] ions in a crystal of complex **II** (Table 1) form infinite chains along axis *b* (Fig. 2c) and also close six- and eight-membered rings (*S*(6) and *R*₂²(8)). The structures of complexes **II** and **I** are stabilized by π–π interaction between Hba[−] anions by the “head-to-head” type [11] with the parameters given in Table 2 [12]. A common structural feature of complexes **I** and **II** is the formation of homotypic six- and twelve-membered rings, chains of Hba[−] ions linked to each other via hydrogen bonds, and similar π–π packings. A distinction appears in the number of metal ions linked to the O(1) and O(2) atoms.

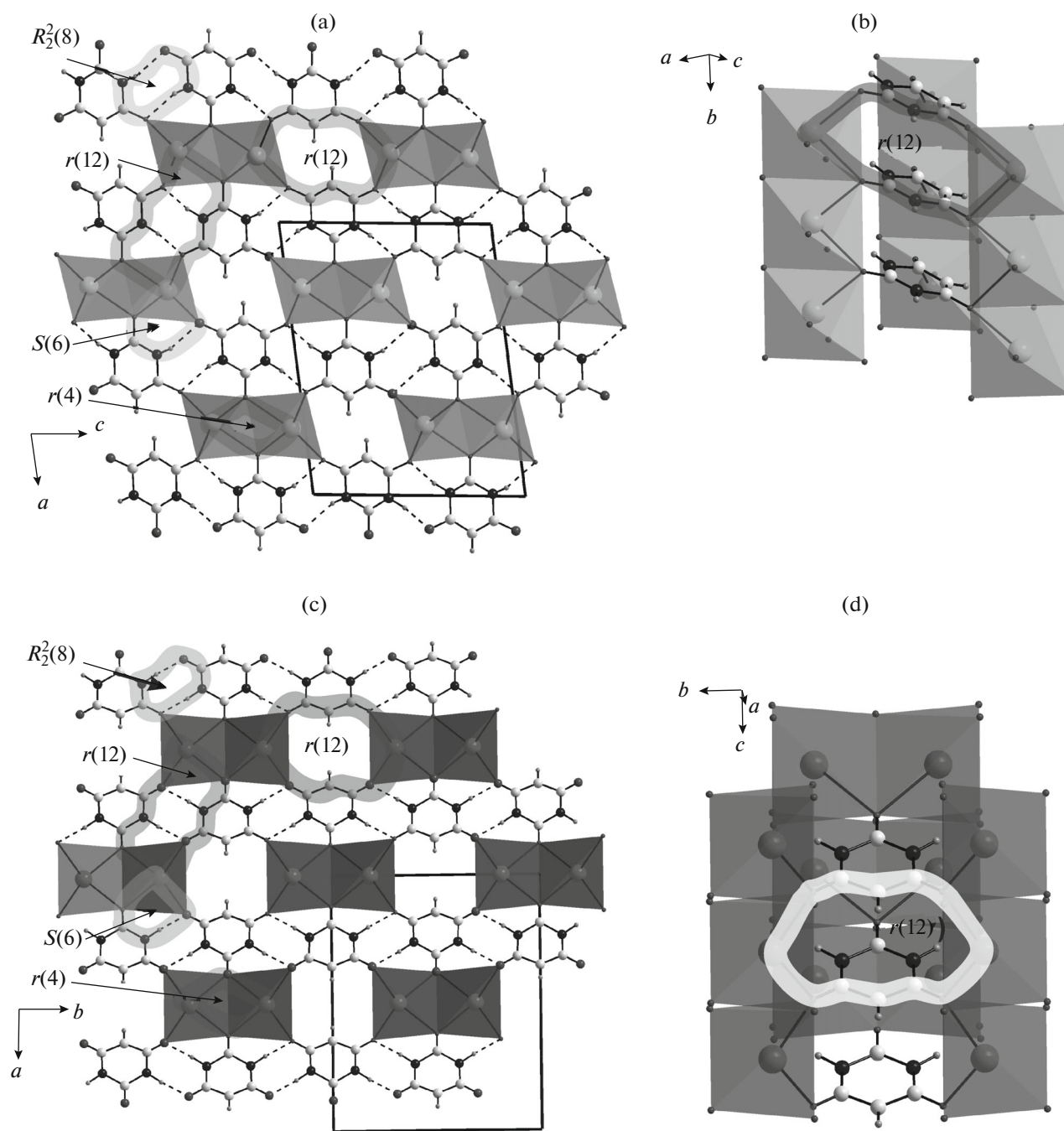


Fig. 2. Three-dimensional framework of KHba in two projections along axes (a) b and (b) $a + c$ and three-dimensional framework of CsHba in two projections along axes (c) c and (d) $a - c$. Dashed lines are hydrogen bonds, and solid lines are structural motifs.

It is of interest to compare the bridging patterns of coordination between an Hba^- ion and a neutral H_2ba molecule in alkali metal complexes. In $[\text{Li}(\text{H}_2\text{O})_2(\text{Hba})]_n$ [9], the only $\mu_2\text{-O, O}'$ -pattern of coordination is implemented for Hba^- . In polymeric salt cocrystals $\text{M}(\text{H}_2\text{ba})\text{X}$ ($\text{M} = \text{Na, K, Rb, Cs}$; $\text{X} = \text{Br, I}$) [13], $\text{M}(\text{H}_2\text{ba})(\text{H}_2\text{O})_2(\text{Hba})$ ($\text{M} = \text{Na, K,}$

$\text{K}(\text{H}_2\text{ba})_{0.5}(\text{H}_2\text{O})_{1.5}(\text{Hba})$ [14], and $\text{Rb}(\text{H}_2\text{ba})(\text{H}_2\text{O})(\text{Hba})$ [15], the terminal coordination mode occurs alongside with the following bridging coordination modes between Hba^- and H_2ba : $\mu_2\text{-O, O}'$, $\mu_2\text{-O, O}$, $\mu_3\text{-O, O, O}'$, $\mu_3\text{-O, O, O}$, $\mu_3\text{-O, O}', \text{O}''$, $\mu_4\text{-O, O, O}', \text{O}''$, $\mu_5\text{-O, O, O}'\text{O}'\text{O}''$. In complexes **I** and **II**, each Hba^- ligand is linked to six metal ions and, in

Table 2. Parameters of π - π interaction between Hba^- ions in the structures of complexes **I** and **II***

Cg_i-Cg_j	$d(Cg-Cg), \text{\AA}$	α, deg	β, deg	γ, deg	$Cg_{i-p}, \text{\AA}$	Shift, \AA
I						
Cg_1-Cg_1'	3.690(3)	0	22.36	22.36	3.412(2)	1.404
II						
Cg_1-Cg_1'	3.81(2)	0	31.00	31.00	3.27(1)	1.962

* Structure of complex **I**: Cg_1 is the N(1), C(2), N(3), C(4), C(5), and C(6) ring plane; Cg_1' is obtained from Cg_1 using the symmetry code $[x, -1 + y, z]$. Structure of complex **II**: Cg_1 is the N(1), N(1'), C(1), C(2), C(2'), and C(5) ring plane; Cg_1' is obtained from Cg_1 using the symmetry code $[x, y, -1 + z]$. Cg_{i-p} is the length of a perpendicular drawn from the center of the i th ring to the plane of the second ring.

contrast to cocrystals, this may be explained by the absence of competitive coordination for halide ions or H_2ba in the process of their formation. In cocrystals $\text{M}(\text{H}_2\text{ba})(\text{H}_2\text{O})_2(\text{Hba})$ ($\text{M} = \text{Na}, \text{K}$) and $\text{K}(\text{H}_2\text{ba})_{0.5}(\text{H}_2\text{O})_{1.5}(\text{Hba})$ [14], the independent K^+ ions have a coordination number $\text{CN} = 8$ or 6. In contrast to cocrystals, KHba contains one type of ligand, and the K^+ ion has an octahedral surrounding.

Topological analysis by the ToposPro software [16] provided the possibility to establish the structural distinction between the frameworks of alkali metal barbiturates in more detail. To accomplish this, Hba^- ions were considered as nodes with coordinates in the gravity center of a molecule. In complex **I**, the K^+ ion is linked to six Hba^- ions, and each Hba^- ion is bonded to six K^+ ions; in addition, the point symbols of these two nodes K^+ and Hba^- turned out to be the same

($4^{12}.6^3$). For this reason, despite the fact that the nodes are chemically different, they are equivalent from the topological viewpoint in our case and, consequently, the network represents a unimodal three-dimensional grid (6), which has the point symbol ($4^{12}.6^3$) and is known as *pcu (alfa-Po)* (Fig. 3a). In complex **II**, the Cs^+ ion is also coordinated to six Hba^- ions, and each Hba^- ion is similarly linked to six Cs^+ ions. Similarly, the Cs^+ and Hba^- nodes are equivalent from the topological viewpoint, but their point symbol ($4^{11}.6^4$) is other than for complex **I**. For this reason, the network in complex **II** represents a unimodal three-dimensional grid (6), which has the point symbol ($4^{11}.6^4$) and is known as *sqc885* (Fig. 3b). This grid of CsHba can be obtained from net *pcu* ($4^{12}.6^3$) of KHba by replacing one of the four-membered rings by a six-membered ring. It seems that a greater ionic radius of Cs^+ ($r(\text{Cs}^+) =$

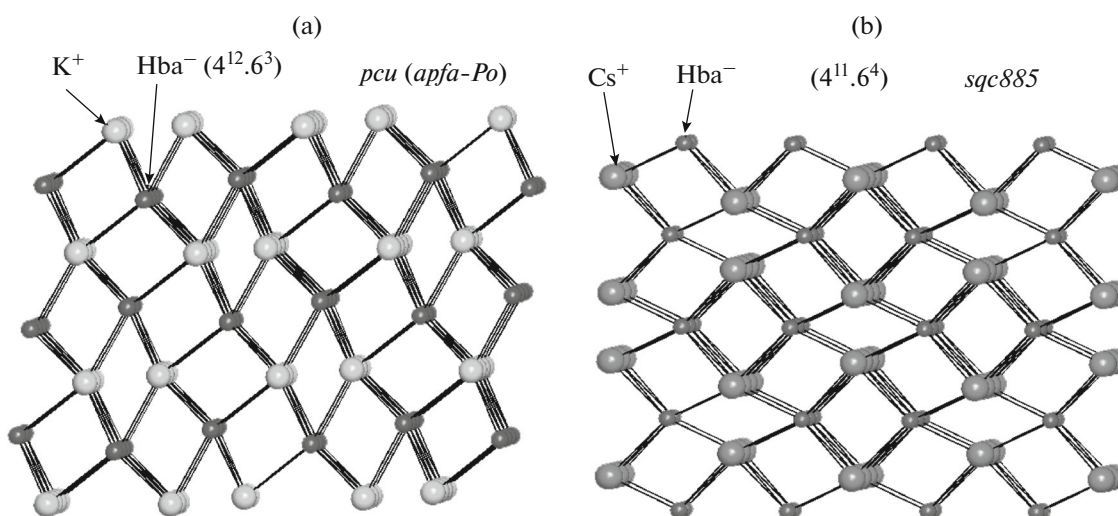


Fig. 3. Topological grids for (a) KHba and (b) CsHba , where the metal ion and the Hba^- anion are nodes located at the gravity centers of ions, with point symbols and topological types.

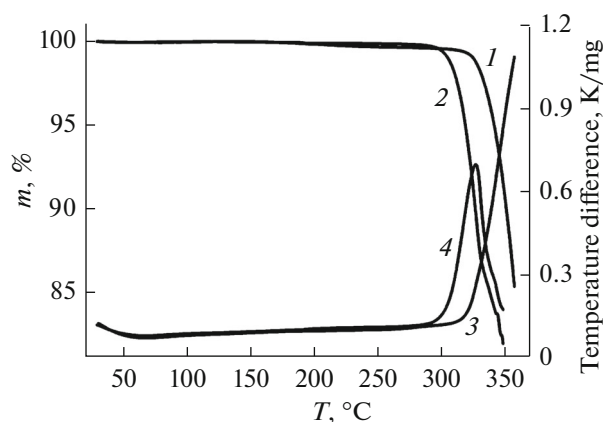


Fig. 4. (1) TG and (3) DSC curves for complex **I** and (2) TG and (4) DSC curves for complex **II** in the course of their decomposition in air.

$1.70 \text{ \AA} > r(\text{K}^+) = 1.38 \text{ \AA}$ [17] favors the formation of larger rings. It should be noted that topology $(4^{12}.6^3)$ was established in the thiobarbiturate complexes KHtba [18] and TIHtba [19] as well as in complex **I**, while RbHtba and CsHtba [20] have topology $(4^{11}.6^4)$ as in complex **II**, though crystals of MHba and MHTba ($M = \text{K, Tl, Rb, Cs}$) are not isostructural. For this reason, an increase in the ionic radius of M^+ from $M = \text{K, Tl}$ to $M = \text{Rb, Cs}$ has led to a change in the topology of barbiturate and thiobarbiturate complexes. However, the complexes MDetba ($M = \text{K, Tl, Rb, Cs}$) [21, 22] have the same topology $(4^{10}.6^5)$ *molI* independent of the ionic radius of M^+ . It is likely that the absence of the effect of M^+ on topology results from that the size of Detba^- is greater than for the Htba^- and Hba^- ions, and the effect produced by the nature of the M^+ ion is not so significant. It should be noted that CsDetba has grid topology $(4^{10}.6^5)$, while the grid topology in complex **II** and CsHtba is $(4^{11}.6^4)$, so the structure of CsDetba contains much less four-membered rings than the structures of complex **II** and CsHtba . Hence, not only a greater size of the M^+ ion, but also a greater size of the ligand hinders the formation of small rings, and the point symbol of grids contains an increasingly great number of rings with a length of >4 nodes. In support of the above interpretation, it is possible to give more examples.

Let us consider another type of network with CN = 3 and 4 in contrast to the previous networks with CN = 6. LiDetba and NaDetba [21] ($r(\text{Li}^+) = 0.59 \text{ \AA}$, $r(\text{Na}^+) = 0.99 \text{ \AA}$ [17]) have grid (4) with point symbol $(4^2.6^4)$, while AgDetba with a greater metal ion radius ($r(\text{Ag}^+) = 1.02 \text{ \AA}$ [17]) has grid $(4^2.6^3.8)$ [23], i.e., contains an additional eight-membered ring instead of a six-membered ring in comparison with $(4^2.6^4)$. On the contrary, the presence of a small-size ligand, e.g., a water molecule, may lead to the formation of a greater num-

ber of four-membered rings. Thus, $\text{M}(\text{H}_2\text{O})_2(\text{Detba})_2$ ($M = \text{Ca, Sr}$) [24] and $\text{M}(\text{H}_2\text{O})_3(\text{Htba})_3$ ($M = \text{Eu, Sm}$) [25, 26] have topological grid $(4^4.6^2)$, in which four-membered rings predominate.

According to TG and DSC curves, complexes **I** and **II** are anhydrous (Fig. 4). In an air atmosphere, complex **I** begins to decompose at $\sim 320^\circ\text{C}$ (Fig. 4, curve 1), while complex **II** is less stable and is subject to oxidative decomposition as soon as at $\sim 300^\circ\text{C}$ (Fig. 4, curve 3). Both complexes are more thermally stable than barbituric acid H_2ba , which melts with decomposition at 245.0°C [10]. The oxidative decomposition of complexes **I** and **II** is accompanied by endotherms at $T > 360$ and $\sim 330^\circ\text{C}$, respectively.

ACKNOWLEDGMENTS

This work was performed within the state task from the Ministry of Education and Science to the Siberian Federal University in 2017–2019 (4.7666.2017/BCh).

REFERENCES

1. R. Ya. Levina and F. K. Velichko, *Usp. Khim.* **29**, 929 (1960).
2. K. T. Mahmudov, M. N. Kopylovich, A. M. Maharramov, et al., *Coord. Chem. Rev.* **265**, 1 (2014).
3. Cambridge Structural Database, Version 5.37 (Cambridge).
4. Bruker AXS TOPAS V4: General profile and structure analysis software for powder diffraction data. User's Manual (Bruker, Karlsruhe, 2008).
5. V. Favre-Nicolin and R. Černý, *J. Appl. Crystallogr.* **35**, 734 (2002).
6. N. N. Golovnev and M. S. Molokeyev, *2-Thiobarbituric Acid and Its Complexes with Metals: Synthesis, Structure, and Properties* (Sib. Feder. Univ., Krasnoyarsk, 2014) [in Russian].
7. N. N. Golovnev, M. S. Molokeyev, and S. N. Vereshchagin, *J. Struct. Chem.* **57**, 167 (2016).
8. N. N. Golovnev, M. S. Molokeyev, and I. I. Golovneva, *Russ. J. Coord. Chem.* **41**, 300 (2015).
9. N. N. Golovnev, M. S. Molokeyev, M. K. Lesnikov, and S. N. Vereshchagin, *Russ. J. Inorg. Chem.* **62**, 746 (2017).
10. N. N. Golovnev, L. A. Solovyov, M. K. Lesnikov, et al., *Inorg. Chim. Acta* **467**, 39 (2017).
11. J. W. Steed and J. L. Atwood, *Supramolecular Chemistry* 1st Ed. (CRC Press, 2004; IKTs Akademkniga, Moscow, 2007).
12. PLATON: A Multipurpose Crystallographic Tool (Utrecht Univ., Utrecht, 2008).
13. D. Braga, F. Grepioni, and L. Maini, *Shem. Commun.* **46**, 7715 (2010).
14. M. R. Chierotti, K. Gaglioti, R. Gobetto, et al., *Cryst. Eng. Commun.* **15**, 7598 (2013).
15. M. Gryl and K. Stadnicka, *Acta Crystallogr., Sect. E* **67**, m571 (2011).

16. V. A. Blatov, A. P. Shevchenko, and D. M. Proserpio, *Cryst. Growth Des.* **14**, 3576 (2014).
17. R. D. Shannon and C. T. Prewitt, *Acta Crystallogr., Sect. B* **25**, 925 (1969).
18. N. N. Golovnev, M. S. Molokeev, and M. Y. Belash, *J. Struct. Chem.* **54**, 566 (2013).
19. N. N. Golovnev and M. S. Molokeev, *Russ. J. Inorg. Chem* **61**, 442 (2016).
20. N. N. Golovnev and M. S. Molokeev, *Russ. J. Inorg. Chem.* **59**, 943 (2014).
21. N. N. Golovnev, M. S. Molokeev, S. N. Vereshchagin, et al., *Polyhedron* **85**, 493 (2015).
22. M. S. Molokeev, N. N. Golovnev, S. N. Vereshchagin, and V. V. Atuchin, *Polyhedron* **98**, 113 (2015).
23. N. N. Golovnev, M. S. Molokeev, and M. A. Lutoshkin, *Russ. J. Inorg. Chem.* **60**, 572 (2015).
24. N. N. Golovnev, M. S. Molokeev, A. S. Samoilov, and V. V. Atuchin, *J. Coord. Chem.* **69**, 957 (2016).
25. N. N. Golovnev and M. S. Molokeev, *Russ. J. Coord. Chem.* **40**, 648 (2014).
26. N. N. Golovnev, M. S. Molokeev, I. V. Sterkhova, et al., *J. Struct. Chem.* **58**, 539 (2017).

Translated by E. Glushachenkova